Available online at www.sciencedirect.com

ScienceDirect

Ceramics International 42 (2016) 5995–5999

CERAMICS INTERNATIONAL

www.elsevier.com/locate/ceramint

Crystal structure and luminescence properties of green-emitting $Sr_{1-x}Al_{12}O_{19}:xEu^{2+}$ phosphors

Bin Ma[a], Qingfeng Guo[a], Maxim S. Molokeev[b,c], Zhenfei Lv[a], Jun Yao[a], Lefu Mei[a], Zhaohui Huang[a,*]

[a]School of Materials Science and Technology, Beijing Key Laboratory of Materials Utilization of Nonmetallic Minerals and Solid Wastes, National Laboratory of Mineral Materials, China University of Geosciences, Beijing 100083, China

[b]Laboratory of Crystal Physics, Institute of Physics, SB RAS, Krasnoyarsk 660036, Russia

[c]Department of Physics, Far Eastern State Transport University, Khabarovsk 680021, Russia

Received 19 November 2015; received in revised form 22 December 2015; accepted 24 December 2015
Available online 4 January 2016

Abstract

In this paper, a series of novel luminescent $Sr_{1-x}Al_{12}O_{19}:xEu^{2+}$ phosphors were synthesized by a high temperature solid-state reaction. The phase structure, photoluminescence (PL) properties, as well as the decay curves were investigated. The quenching concentration of Eu^{2+} in $SrAl_{12}O_{19}$ was about 0.15 (mol). Upon excitation at 378 nm, the composition-optimized $Sr_{0.85}Al_{12}O_{19}:0.15Eu^{2+}$ exhibited strong broad-band green emission at 530 nm with the CIE chromaticity (0.2917, 0.5736). The results indicate that $Sr_{1-x}Al_{12}O_{19}:xEu^{2+}$ phosphors have potential applications as green-emitting phosphors for UV-pumped white-light LEDs.

Keywords: Crystal structure; Magnetoplumbite; Phosphor

1. Introduction

White light emitting diodes (*w*-LEDs) solid-state lighting technology has been widely used and attracted lots of research interests due to their promising features, such as low power consumption, high efficiency, as well as environmental friendliness characteristics [1–3]. To the best of our knowledge, the typical *w*-LEDs can be obtained by a combination of the blue LEDs with yellow emission from the $Y_3Al_5O_{12}:Ce^{3+}$ (YAG:Ce) phosphors [4,5]. However, these phosphors are suffering from some disadvantages such as poor color-rendering index and high correlated color temperature caused by the weak red emission. Therefore, it is necessary to introduce bright tricolor (red, green, and blue) phosphors for the development of tricolor emission phosphors upon *n*-UV light (350–420 nm) [6,7]. Eu^{2+} ion is more sensitive to the crystal field and covalence for its $4f$–$5d$ transition, and Eu^{2+}-doped phosphor generally has superior absorption in the spectral region of 250–400 nm, which is equivalent with the emission of UV and *n*-UV LED chip, and they also exhibit broad emission bands from blue to red [8,9]. Many efforts to develop new *w*-LEDs phosphors in order to address issues of higher efficiency, better color rendition and better chemical and thermal stability [10–12]. As we know, the rare earth ions plays an important and irreplaceable role in lighting and display fields for their $4f \rightarrow 4f$ or $5d \rightarrow 4f$ transitions. In addition, Eu^{2+} is a kind of important activator ions among rare earth ions for novel phosphors showing a wide range of emission because of $4f^6 5d^1 \rightarrow 4f^7$ transition, resulting from that the $5d$ orbital of Eu^{2+} in the outer space are more sensitive to the crystal field environment [13–15]. Therefore, it is important and necessary to find a host with a specific crystal field to accommodate Eu^{2+} ions.

Strontium aluminates are considered for use as one of phosphor host materials and have been widely studied in

*Corresponding author. School of Materials Science and Technology, China University of Geosciences, Beijing 100083, China.
Tel./fax: +86 10 82322186.
E-mail address: huang118@cugb.edu.cn (Z. Huang).

http://dx.doi.org/10.1016/j.ceramint.2015.12.149
0272-8842/

many fields because of their outstanding properties, such as safety, good stability, and high quantum efficiency [16]. Strontium aluminates structured in a variety of stoichiometries, for example: $SrAl_{12}O_{19}$, $Sr_4Al_{14}O_{25}$, $Sr_3Al_2O_6$, $SrAl_2O_4$ and $SrAl_4O_7$ [17]. Among them, there have been investigations concerning the $Sr_{1-x}Al_{12}O_{19}:xEu^{2+}$ phosphors in the literatures. However, most papers focus on energy transfers between Eu^{2+} and other ions, and the $Sr_{1-x}Al_{12}O_{19}:xEu^{2+}$ phosphors were mainly prepared not by solid state reaction [18–22]. Dutczak stylized prepared a series of strontium aluminates phosphors using a two-step solid state reaction, and the emission spectra of $SrAl_{12}O_{19}:Eu^{2+}$ at 4 K and 300 K were studied. However, the research focuses to explain the strong emission color variation of different strontium aluminates [17].

As we know, no details on crystal structure, quenching concentration, and quenching mechanism of Eu^{2+} ions in $SrAl_{12}O_{19}$ were reported in the previous literatures so far. As such, in this paper, $SrAl_{12}O_{19}:Eu^{2+}$ phosphors were prepared via a one-step solid state reaction, as well as the quenching concentration and mechanism of Eu^{2+} ions in $SrAl_{12}O_{19}$ were also discussed in detail. In addition, Rietveld refinement of the selected $Sr_{0.94}Al_{12}O_{19}:0.06Eu^{2+}$ and $Sr_{0.92}Al_{12}O_{19}:0.08Eu^{2+}$ samples were performed in detail. All the results indicated that the $Sr_{1-x}Al_{12}O_{19}:xEu^{2+}$ phosphors can be potentially applied as the green-emitting component in *w*-LEDs.

2. Experimental procedure

2.1. Materials and synthesis

$Sr_{1-x}Al_{12}O_{19}:xEu^{2+}$ phosphors were synthesized by a traditional high temperature solid-state reaction method. Stoichiometric amounts of raw materials $SrCO_3$ (Aldrich, 99.9%), Al_2O_3 (Aldrich, 99.9%), and Eu_2O_3 (A. R.) were weighed and mixed by grinding in an agate mortar. The mixture were placed into alumina crucibles and annealed at 1500 °C in a reducing atmosphere in flowing gas (10% H_2+90% N_2) for 5 h. After firing, the samples were gradually cooled to room temperature in the furnace. The products were crushed and finally obtained for measurements.

2.2. Characterization methods

The phase structures of the as-prepared samples were checked by X-ray powder diffractometer (D/max-rA 12kw, Japan) with Cu Kα radiation (λ=1.5418 Å) from 3° to 90° (2θ). The step scanning rate (2θ values ranging from 10° to 120°) used for Rietveld analysis was 2 *s/step* with a step size of 0.02°. Rietveld refinement of the structure of the select $Sr_{0.94}Al_{12}O_{19}:0.06Eu^{2+}$ and $Sr_{0.92}Al_{12}O_{19}:0.08Eu^{2+}$ samples were performed by using the computer software TOPAS [23]. Room temperature photoluminescence excitation (PLE) and emission (PL) spectra were measured on a fluorescence spectrophotometer (F-4600, HITACHI, Japan) with a photomultiplier tube operating at 600 V, and a 150 W Xe lamp was used as the excitation lamp. The decay curves of Eu^{2+} lifetime values were recorded at room temperature on a spectrofluorometer (HORIBA JOBIN YVON FL3-21), and the 370 nm pulse laser radiation (370-nm Nano LED, model number 08254) was used as the excitation source.

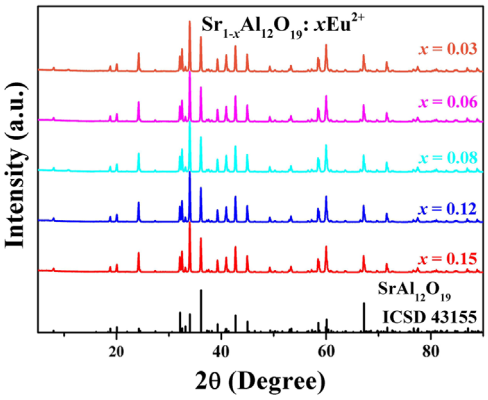

Fig. 1. The XRD patterns of $Sr_{1-x}Al_{12}O_{19}:xEu^{2+}$ phosphors (x=0.03, 0.06, 0.08, 0.12, and 0.15) and the standard $SrAl_{12}O_{19}$ (ICSD no. 43155) is shown as a reference.

3. Results and discussion

3.1. Phase purity and structure

Fig. 1 shows the XRD patterns of $Sr_{1-x}Al_{12}O_{19}:xEu^{2+}$ phosphors (x=0.03, 0.06, 0.08, 0.12, and 0.15) and the standard $SrAl_{12}O_{19}$ (ICSD no. 43155) [24] is shown as a reference. As shown in Fig. 1, the XRD patterns of all the $Sr_{1-x}Al_{12}O_{19}:xEu^{2+}$ samples can be exactly assigned to $SrAl_{12}O_{19}$ (ICSD no. 43155). What is more, no second phase is observed in the XRD patterns of all the $Sr_{1-x}Al_{12}O_{19}:xEu^{2+}$ phosphors. Based on the charge balance and similarity of ion radii, Eu^{2+} ions prefer to occupy the sites of Sr^{2+}. In order to better understand the crystallographic sites of Eu^{2+} in $SrAl_{12}O_{19}$ lattice, the powder diffraction data of the select $Sr_{0.94}Al_{12}O_{19}:0.06Eu^{2+}$ and $Sr_{0.92}Al_{12}O_{19}:0.08Eu^{2+}$ samples for Rietveld analysis were collected at room temperature. Rietveld refinement was performed by using TOPAS 4.2. It can be found that almost all peaks were indexed by hexagonal cell ($P6_3/mmc$) with parameters close to $SrAl_{12}O_{19}$ (magnetoplumbite-type structure). Therefore crystal structure of $SrAl_{12}O_{19}$ was taken as starting model for Rietveld refinement. Site of Sr^{2+} ion was occupied by Eu^{2+} ions with fixed occupation according to suggested formula. Refinements were stable and give low *R*-factors, as shown in Table 1 and Fig. 2. The reliability parameters goodness of fitting (*GOF*) of refinement are *GOF*=1.94 and 1.66 for $Sr_{0.94}Al_{12}O_{19}:0.06Eu^{2+}$ and $Sr_{0.92}Al_{12}O_{19}:0.08Eu^{2+}$. Small reliability parameters (Table 1) also verify the phase purity of the as-prepared samples. In addition, cell volume in the two compounds decreases with increasing of x, which is consistent with smaller ion radii of Eu^{2+} in comparison with Sr^{2+} (590.96 $Å^3$ for $Sr_{0.94}Al_{12}O_{19}:0.06Eu^{2+}$ and 590.90 $Å^3$ for $Sr_{0.92}Al_{12}O_{19}:0.08Eu^{2+}$).

3.2. Luminescence properties

Fig. 3 presents the photoluminescence excitation (PLE) and photoluminescence (PL) spectra of the as-prepared $Sr_{0.85}Al_{12}O_{19}$:$0.15Eu^{2+}$ phosphor. It can be seen that the PLE spectrum of the phosphor has a broad absorption centered at 378 nm with a wide range from 250 to 500 nm attributed to the 4*f*–5*d* transitions of Eu^{2+} ions. Besides, the PL spectrum exhibits a green emission band peaked at 530 nm under the excitation at 378 nm.

Fig. 4 displays the PL spectra of $Sr_{1-x}Al_{12}O_{19}$:xEu^{2+} phosphors (x=0.03, 0.06, 0.08, 0.12, 0.15, and 0.18) under 378 nm light excitation. The result indicated that the optimal doping concentration of Eu^{2+} in $SrAl_{12}O_{19}$ host was 0.15 mol. It can be easily seen that the PL intensity would decrease when the concentration exceeds the critical concentration, which is caused by the concentration quenching effect. What is more, the critical energy transfer distance R_C between Eu^{2+} ions in $SrAl_{12}O_{19}$ can be estimated by using concentration quench equation proposed by Blasse [25,26]:

$$R_C \approx 2\left[\frac{3V}{4\pi x_c N}\right]^{1/3} \quad (1)$$

where V is for the volume of the unit cell, x_c stands the atom fraction of activator at which the quenching occurs, and N represents the number of host cations in the unit cell. For the $SrAl_{12}O_{19}$ host, there are two Sr ions in whole unit cell, and they are linked by symmetry elements, so N should be equal to 2. Only asymmetric part of unit cell has one Sr ion, but this part of unit cell has volume equal to 588.65/Z=588.65/2=294.33 Å^3, and x_c is 0.15 for emission peak at 530 nm. Thus, the critical distances R_C of energy transfer can be estimated to be about 12.33 Å (x_c=0.15) by using Eq. (1). As is known to us, the non-radiative transitions between Eu^{2+} ions took place via electric multipolar interactions with R_C

Table 1
Main parameters of processing and refinement of $Sr_{0.94}Al_{12}O_{19}$:$0.06Eu^{2+}$ and $Sr_{0.92}Al_{12}O_{19}$:$0.08Eu^{2+}$ samples.

Compound	$Sr_{0.94}Al_{12}O_{19}$:$0.06Eu^{2+}$	$Sr_{0.92}Al_{12}O_{19}$:$0.08Eu^{2+}$
Space Group	*P*6$_3$/*mmc*	*P*6$_3$/*mmc*
a, Å	5.56841 (8)	5.56801 (8)
c, Å	22.0070 (3)	22.0081 (3)
V, Å^3	590.96 (2)	590.90 (2)
Z	2	2
2*θ*-interval, °	5–100	5–100
No. of reflections	153	153
R_{wp}, %	8.47	7.34
R_p, %	6.06	5.34
R_{exp}, %	4.37	4.42
χ^2	1.94	1.66
R_B, %	2.81	2.82

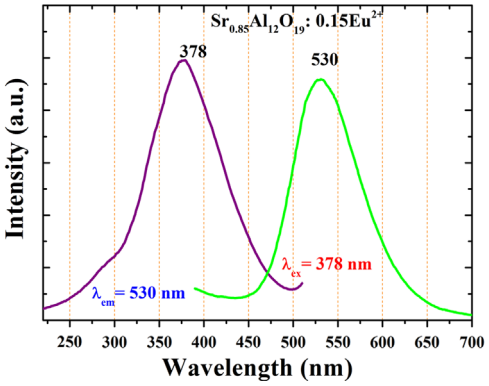

Fig. 3. PLE (left) and PL (right) spectrum of the selected $Sr_{0.85}Al_{12}O_{19}$:0.15 Eu^{2+} sample.

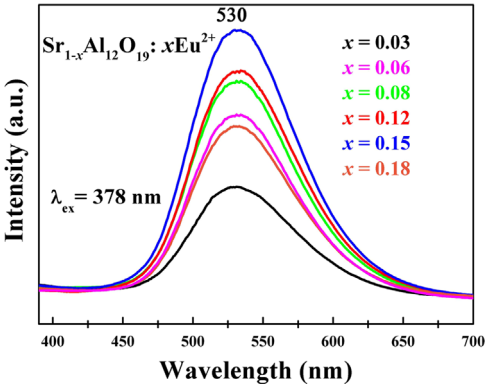

Fig. 4. The PL spectra of $Sr_{1-x}Al_{12}O_{19}$:xEu^{2+} (x=0.03, 0.06, 0.08, 0.12, 0.15, and 0.18) phosphors under 378 nm excitation.

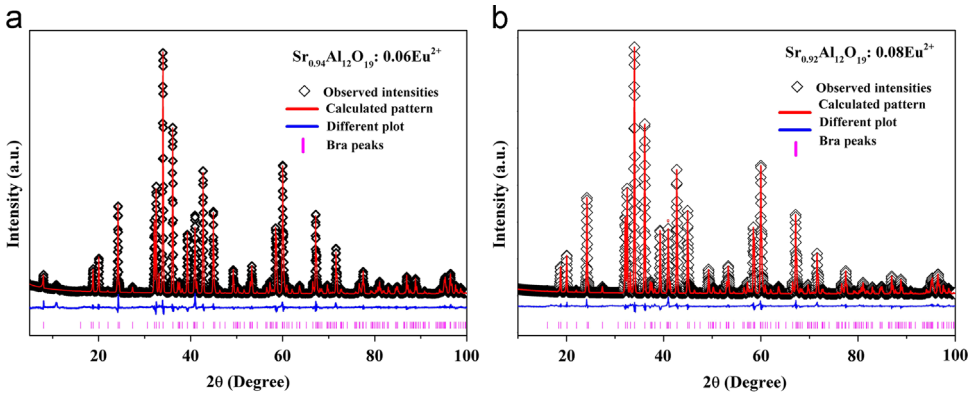

Fig. 2. Rietveld analysis patterns for X-ray powder diffraction data of $Sr_{0.94}Al_{12}O_{19}$:$0.06Eu^{2+}$ (a) and $Sr_{0.92}Al_{12}O_{19}$:$0.08Eu^{2+}$ (b).

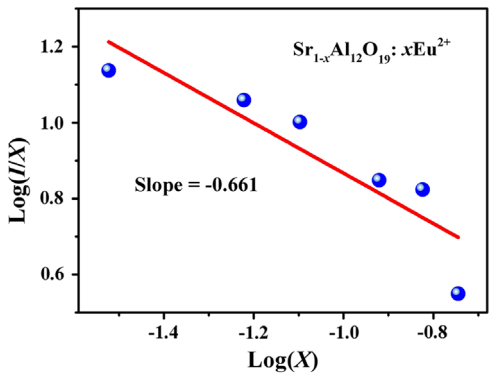

Fig. 5. The fitting line of log(*I*/*x*) vs. log(*x*) in $Sr_{1-x}Al_{12}O_{19}:xEu^{2+}$ phosphor beyond the quenching concentration.

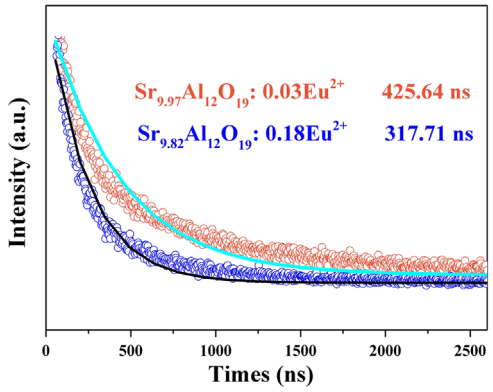

Fig. 6. The decay curves and lifetime of Eu^{2+} in the selected $Sr_{0.97}Al_{12}O_{19}:0.03Eu^{2+}$ $Sr_{0.82}Al_{12}O_{19}:0.18Eu^{2+}$ phosphors monitored at 530 nm at room temperature.

more than 5 Å according to the Dexter theory. Moreover, the interaction type between sensitizers or between sensitizer and activator can be calculated by the following equation [27–29]:

$$\frac{I}{x} = K\left[1+\beta(x)^{\frac{\theta}{3}}\right]^{-1} \quad (2)$$

where I is the emission intensity, x stands for the activator concentration, k and β are constants for each type of interaction for a given host lattice, and θ is an indication of electric multipolar character. In general, $\theta=6$, 8, 10 can be assigned to dipole–dipole (*d*–*d*), dipole-quadrupole (*d*–*q*), quadrupole-quadrupole (*q*–*q*) interactions, respectively. Fig. 5 illustrates the fitting line of log(*I*/*x*) vs. log(*x*) in $Sr_{1-x}Al_{12}O_{19}:xEu^{2+}$ phosphors for the emission peak of 530 nm beyond the quenching concentration. The fitting line was found to be relatively linear with a slope equal to $-\theta/3$, and the slope was determined to be -0.661. Therefore, the value of θ can be calculated to be 1.983, which is less than 6. Therefore, the quenching is dipole–dipole interactions in $Sr_{1-x}Al_{12}O_{19}:xEu^{2+}$ phosphors.

The decay curves and lifetime of Eu^{2+} in the selected $Sr_{0.97}Al_{12}O_{19}:0.03Eu^{2+}$ $Sr_{0.82}Al_{12}O_{19}:0.18Eu^{2+}$ phosphors monitored at 530 nm at room temperature are shown in Fig. 6. It can be seen that the decay curves of Eu^{2+} in the two

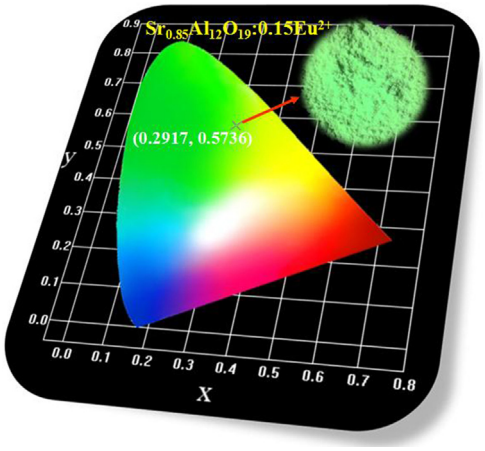

Fig. 7. Color coordinates of $Sr_{0.85}Al_{12}O_{19}:0.15Eu^{2+}$ in the CIE chromaticity diagram, and the inset shows a digital photograph of the green-emitting phosphor excited at 365 nm.

phosphors can be best fitted using the double exponential equation.:

$$I = A_1\, exp\left(-t/\tau_1\right) + A_2 exp\left(-t/\tau_2\right) \quad (3)$$

where I is the luminescence intensity, t is the time, A_1 and A_2 represent constants, and τ_1 and τ_2 are decay constants of exponential aspects [30]. The average lifetime τ^* can be obtained by the formula as follows:

$$\tau * = (A_1\tau_1{}^2 + A_2\tau_2{}^2)/(A_1\tau_1 + A_2\tau_2) \quad (4)$$

The double exponential decay curves indicate the possible interactions between Eu^{2+} ions. On the basis of Eqs. (3) and (4), the lifetime values of Eu^{2+} were determined to be 425.64 and 317.71 ns $Sr_{0.97}Al_{12}O_{19}:0.03Eu^{2+}$ $Sr_{0.82}Al_{12}O_{19}:0.18Eu^{2+}$, respectively. Thus, the decreasing lifetime of the $4f^6 5d \rightarrow 4f^7$ transition with the increasing Eu^{2+} ions concentrations further exhibits the trend of the energy transfer between Eu^{2+} ions in the $SrAl_{12}O_{19}$ lattice.

CIE chromaticity coordinates (*x*, *y*) of the $Sr_{0.85}Al_{12}O_{19}:0.15Eu^{2+}$ sample upon 378 nm excitation calculated through its PL spectrum and the digital image of the sample under 365 nm UV lamp excitation are shown in Fig. 7. The color coordinate is calculated to be (0.2917, 0.5736). Besides, the phosphor shows intense green emission as shown in the inset of Fig. 7. Therefore, this phosphor can be used as a green-emitting phosphor for *n*-UV *w*-LEDs.

4. Conclusions

In summary, magnetoplumbite structure phosphors $Sr_{1-x}Al_{12}O_{19}:xEu^{2+}$ have been synthesized and investigated in this paper. The $Sr_{1-x}Al_{12}O_{19}:xEu^{2+}$ phosphor exhibits a broad-band green emission at 530 nm under the excitation at 378 nm. In addition, $Sr_{1-x}Al_{12}O_{19}:xEu^{2+}$ shows strong and broad absorption in the near UV regions and the optimum excitation band locates in the 250–500 nm region. Eu^{2+} can occupy the Sr1 site in $SrAl_{12}O_{19}$. In addition, the dipole–dipole interactions results in the concentration quenching of Eu^{2+} in $Sr_{1-x}Al_{12}O_{19}:xEu^{2+}$. The above results demonstrate

the $Sr_{1-x}Al_{12}O_{19}:xEu^{2+}$ phosphor can be used as green emitting phosphor in the *w*-LEDs.

Acknowledgments

This work was supported by the National Natural Science Foundation of China (Grant nos. 51032007 and 51372232) and the Fundamental Research Funds for the Central Universities (Grant no. 2652015024).

References

[1] Q. Xu, D. Xu, J. Sun, Preparation and luminescence properties of orange-red $Ba_3Y(PO_4)_3$: Sm^{3+} phosphors, Opt. Mater. 42 (2015) 210–214.

[2] Q. Guo, L. Liao, L. Mei, H. Liu, Y. Hai, Color-tunable photoluminescence phosphors of Ce^{3+} and Tb^{3+} co-doped $Sr_2La_8(SiO_4)_6O_2$ for UV w-LEDs, J. Solid State Chem. 225 (2015) 149–154.

[3] K. Li, J. Fan, X. Mi, Y. Zhang, H. Lian, M. Shang, J. Lin, Tunable-color luminescence via energy transfer in $NaCa_{13/18}Mg_{5/18}PO_4$:A (A=$Eu^{2+}$/$Tb^{3+}$/$Mn^{2+}$, Dy^{3+}) phosphors for solid state lighting, Inorg. Chem. 53 (2014) 12141–12150.

[4] K.M. Kim, J.H. Ryu, Synthesis of $Y_3Al_5O_{12}:Ce^{3+}$ colloidal nanocrystals by pulsed laser ablation and their luminescent properties, J. Alloy. Compd. 576 (2013) 195–200.

[5] Z. Zhou, S. Liu, F. Wang, Y. Liu, Synthesis of $Y_3Al_5O_{12}:Ce^{3+}$ phosphors by a modified impinging stream method: a crystal growth and luminescent properties study, J. Phy. D. Appl. Phys. 45 (2012) 1–8.

[6] Z. y Mao, Y. c Zhu, Y. Wang, L. Gan, Ca_2SiO_4:Ln (Ln=Ce^{3+}, Eu^{2+}, Sm^{3+}) tricolor emission phosphors and their application for near-UV white light-emitting diode, J. Mater. Sci. 49 (2014) 4439–4444.

[7] C.H. Huang, T.M. Chen, W.-R. Liu, Y.C. Chiu, Y.T. Yeh, S.M. Jang, A. Single-Phased Emission-Tunable, Phosphor $Ca_9Y(PO_4)_7:Eu^{2+},Mn^{2+}$ with efficient energy transfer for white-light-emitting diodes, ACS Appl. Mater. Interfaces 2 (2010) 259–264.

[8] G. Bizarri, B. Moine, On the role of traps in the $BaMgAl_{10}O_{17}:Eu^{2+}$ fluorescence mechanisms, J. Lumin. 115 (2005) 53–61.

[9] Q. Guo, L. Liao, L. Mei, H. Liu, Crystal structure, thermally stability and photoluminescence properties of novel $Sr_{10}(PO_4)_6O:Eu^{2+}$ phosphors, J. Solid State Chem. 226 (2015) 107–113.

[10] C. Peng, G. Li, Z. Hou, M. Shang, J. Lin, Electrospinning synthesis and luminescent properties of one-dimensional $Ca_2Gd_8(SiO_4)_6O_2:Eu^{3+}$ microfibers and microbelts, Mater. Chem. Phys. 136 (2012) 1008–1014.

[11] W. Lv, M. Jiao, Q. Zhao, B. Shao, W. Lu, H. You, $Ba_{1.3}Ca_{0.7}SiO_4:Eu^{2+}$, M^{n2+}: a promising single-phase, color-tunable phosphor for near-ultraviolet white-light-emitting diodes, Inorg. Chem. 53 (2014) 11007–11014.

[12] R. Pang, C. Li, L. Shi, Q. Su, A novel blue-emitting long-lasting proyphosphate phosphor $Sr_2P_2O_7:Eu^{2+},Y^{3+}$, J. Phys. Chem. Solids, 70, 2009, p. 303–306.

[13] X. Zhao, Z. Li, T. Yu, Z. Zou, Tunable orange red phosphors: S^{2-} doped high temperature phase $Ca_3SiO_4Cl_2:Eu^{2+}$ for solid-state lighting, RSC Adv. 3 (2013) 1965–1969.

[14] C. Zhao, Z. Xia, S. Yu, Thermally stable luminescence and structure evolution of (K, Rb)$BaPO_4:Eu^{2+}$ solid-solution phosphors, J. Mater. Chem. C, 2, 2014, p. 6032–6039.

[15] S.J. Gwak, P. Arunkumar, W.B. Im, A new blue-emitting oxohalide phosphor $Sr_4OCl_6:Eu^{2+}$ for thermally stable, efficient white-light-emitting devices under near-UV, J. Phys. Chem. C 118 (2014) 2686–2692.

[16] S. Yeşilay Kaya, E. Karacaoglu, B. Karasu, Effect of Al/Sr ratio on the luminescence properties of $SrAl_2O_4:Eu^{2+}$, Dy^{3+} phosphors, Ceram. Int., 38, , 2012, p. 3701–3706.

[17] D. Dutczak, T. Justel, C. Ronda, A. Meijerink, Eu^{2+} luminescence in strontium aluminates, Phys. Chem. Chem. Phys. 17 (2015) 15236–15249.

[18] V. Singh, T.K. Gundu Rao, J.J. Zhu, Preparation, luminescence and defect studies of Eu^{2+}-activated strontium hexa-aluminate phosphor prepared via combustion method, J. Solid State Chem. 17 (2006) 2589–2594.

[19] J.S. Choi, S.H. Baek, S.G. Kim, S.H. Lee, H.L. Park, S.-I. Mho, T. W. Kim, Y.H. Hwang, Energy transfer between Ce^{3+} and Eu^{2+} in $SrAl_{12}O_{19}:Ce_x^{3+},Eu_{0.01}^{2+}$ (x=0.01–0.09), Mater. Res. Bull. 34 (1999) 551–556.

[20] R.X. Zhong, J.H. Zhang, X. Zhang, S.Z. Lu, X.J. Wang, Efficient energy transfer and photoluminescent characteristics in $SrAl_{12}O_{19}:Eu^{2+}$, Cr^{3+} nano-rods, Nanotechnology 18 (2007) 1–5.

[21] S. Chawla, A. Yadav, Role of valence state of dopant (Eu^{2+}, Eu^{3+}) and growth environment in luminescence and morphology of $SrAl_{12}O_{19}$ nano- and microcrystals, Mater. Chem. Phys. 122 (2010) 582–587.

[22] K. Komatsu, S. Tsuchida, H. Maruyama, S. Ohshio, H. Akasaka, H. Saitoh, Synthesis of a violet Sr–Al–O:Eu^{2+} phosphor particle using elemental Al diffusion, Int. J. Appl. Ceram. Technol. 11 (2014) 594–601.

[23] A.X.S. Bruker, TOPAS V4: General profile and structure analysis software for powder diffraction data – User's Manual, Bruker AXS, Karlsruhe, Germany, 2008.

[24] J.G. Park, A. Cormack, Crystal/defect structures and phase stability in Ba hexaaluminates, J. Solid State Chem. 121 (1996) 278–290.

[25] G. Blasse, Energy transfer in oxidic phosphors, Phys. Lett. A 28 (1968) 444–445.

[26] G. Blasse, Energy transfer between inequivalent Eu^{2+} ions, J. Solid State Chem. 62 (1986) 207–211.

[27] S. Miao, Z. Xia, J. Zhang, Q. Liu, Increased Eu^{2+} content and codoping Mn^{2+} induced tunable full-color emitting phosphor $Ba_{1.55}Ca_{0.45}SiO_4:Eu^{2+},Mn^{2+}$, Inorg. Chem. 53 (2014) 10386–10393.

[28] Y. Chen, Y. Li, J. Wang, M. Wu, C. Wang, Color-tunable phosphor of Eu^{2+} and Mn^{2+} codoped $Ca_2Sr(PO_4)_2$ for UV light-emitting diodes, J. Phys. Chem. C 118 (2014) 12494–12499.

[29] W. Lv, Y. Jia, Q. Zhao, W. Lu, M. Jiao, B. Shao, H. You, Synthesis, structure, and luminescence properties of $K_2Ba_7Si_{16}O_{40}:Eu^{2+}$ for white light emitting diodes, J. Phys. Chem. C 118 (2014) 4649–4655.

[30] D. Geng, H. Lian, M. Shang, Y. Zhang, J. Lin, Oxonitridosilicate $Y_{10}(Si_6O_{22}N_2)O_2:Ce^{3+},Mn^{2+}$ phosphors: a facile synthesis via the soft-chemical ammonolysis process, luminescence, and energy-transfer properties, Inorg. Chem. 53 (2014) 2230–2239.